Chinese Chemical Letters 32 (2021) 557–560

Contents lists available at ScienceDirect

Chinese Chemical Letters

journal homepage: www.elsevier.com/locate/cclet

Communication

Two isostructural Ni(II)/Co(II)-based metal-organic frameworks for selective dye adsorption and catalytic cycloaddition of CO_2 with epoxides

Hui Hu[a,1], Dashuai Zhang[a,1], Huiling Liu[a], Yaoqiang Jin[a,c], Jun Gao[d], Yongzheng Zhang[a], Zhongmin Liu[a], Xiuling Zhang[a,c,**], Longlong Geng[a,**], Suijun Liu[b,*], Ranhui Zhang[a,c]

[a] College of Chemistry and Chemical Engineering, Dezhou University, Dezhou 253023, China
[b] School of Chemistry and Chemical Engineering, Jiangxi University of Science and Technology, Ganzhou 341000, China
[c] College of Chemical Engineering, Qingdao University of Science and Technology, Qingdao 266000, China
[d] College of Chemical and Environmental Engineering, Shandong University of Science and Technology, Qingdao 266590, China

ARTICLE INFO

Article history:
Received 10 February 2020
Received in revised form 12 February 2020
Accepted 12 February 2020
Available online 14 February 2020

Keywords:
Metal-organic frameworks
Dye separation
Heterogeneous catalysis
CO_2 cycloaddition
Coordination polymers

ABSTRACT

Two isostructural Ni(II)/Co(II)-based metal-organic frameworks (MOFs), namely $\{[M_3(L)_2(bpb)_3(H_2O)_4]\cdot 2DMF\cdot 2H_2O\}_n$ [M = Ni (**HL-5**, HL is short for Hui-Ling Liu); M = Co (**HL-6**); H_3L = 2′,6′-dimethyl-[1,1′-biphenyl]-3,4′,5-tricarboxylic acid; bpb = 1,4-bis(pyrid-4-yl)benzene], have been hydrothermally synthesized and structurally characterized. Both **HL-5** and **HL-6**, which have the same three-interpenetrated 3D pillared-layer framework with *sqc306* type topology, present good selective methyl orange (MO) adsorption over rhodamine B (RhB). Moreover, the catalytic CO_2 cycloaddition properties with epoxides of the two MOFs have also been studied at ambient pressure and temperature.

Nowadays, the environment deterioration has been one of the biggest issues which is unable to avoid. For example, the release of toxic organic compounds or harmful gases have seriously endangered the ecological balance and brought a variety of disasters and diseases to human beings. To solve these problems, many ideas have been developed, based on the keywords of *degradation*, *adsorption* or *conversion* [1–3]. Therefore, how to degrade, adsorb, separate or convert these hazardous wastes is of great significance and challenge, and to realize this purpose, one of the important directions is exploit relative materials that could efficiently deal with these pollutants.

Recently, porous metal-organic frameworks (MOFs), which are composed of inorganic metal centers and organic ligands, have received great attention since this kind of materials entered the sight of human. Compared with many traditional materials, MOFs have presented many unique physical and chemical properties, and showed potential applications in lots of areas (*e.g.*, storage, separation, catalysis and sensing) [4–21]. The micro/meso-porosity of MOFs make them very suitable for the adsorption of specific molecules (*e.g.*, gas or organics) [22–26]; through the modulation of ligands and/or metal centers, the pores of MOFs could be easily functionalized and size/shape-modulated, which further brought excellent performances such as molecule sieving and selective catalysis [27–33]. All these features confirm that MOFs are well in line with the concept mentioned above in this area, and some success have also been achieved in designing MOFs with excellent performances for pollutant removal and transformation [34–38]. However, some non-ignored problems also need to be solved, for example, the framework stability towards hard conditions (many MOFs lost their porosity when degassed, exposed in water or under high temperature due to their weak coordination bonds). Therefore, there is still a long way to go for the studies of this field.

In this work, our focus lies on the dye adsorption and CO_2 conversion. Here, we present two isostructural Ni(II)/Co(II)-based MOFs, namely $\{[M_3(L)_2(bpb)_3(H_2O)_4]\cdot 2DMF\cdot 2H_2O\}_n$ [M = Ni (**HL-5**); M = Co (**HL-6**)], with a three-fold interpenetrated *sqc306* type topology. Due to their interpenetrated features, both the two MOFs exhibit excellent hydrothermal stabilities. Moreover, **HL-5** and **HL-6** shows good bifunctions in selective dye adsorptions and catalytic cycloaddition of CO_2 with epoxides.

* Corresponding author.
** Corresponding authors at: College of Chemistry and Chemical Engineering, Dezhou University, Dezhou 253023, China.
E-mail addresses: xlzhang99@126.com (X. Zhang), llgeng@126.com (L. Geng), sjliu@jxust.edu.cn (S. Liu).
[1] These authors contributed equally to this work.

https://doi.org/10.1016/j.cclet.2020.02.028
1001-8417/

Single-crystal diffraction analysis reveals the two MOFs are isostructural in spite of their different metal centers and space groups (**HL-5**: Ni^{2+}, *C*2/*m*; **HL-6**: Co^{2+}, $P\bar{1}$). Therefore, in the following description, **HL-6** is selected to show their structures. As illustrated in Fig. S1b (Supporting information), the asymmetric unit of **HL-6** contains three Co(II) centers (Co1, Co2, and Co3), one L^{3-} ligand, three bpb ligands and two water molecules. All Co(II) ions are six-coordinated (two N atoms and four O atoms) with octahedral geometry (Table S2 in Supporting information) calculated by *SHAPE 2.1* [39] and two vertexes of the octahedron are occupied by the two N atoms from different bpb ligands with four O atoms forming the equatorial plane. However, for Co1 and Co2, coordinated O atoms are from two isophthalate groups of L^{3-} ligands and two water molecules, while for Co3, the four O atoms are all from the third carboxylate groups of two different L^{3-} ligands. The Co—O bond distances are from 2.081(2) Å to 2.140(2) Å, and the Co—N bonds range from 2.102(3) Å to 2.159(3) Å. In addition, the coordination angles around Co(II) ions are in the range of 61.33(10)°–180.0° (Table S3 in Supporting information). Each L^{3-} ligand acting as a 3-connected linker in a μ_3-η^1:η^1:η^2 coordination mode (two monodentate and one chelate, Fig. S1c in Supporting information), connects three Co(II) ions, resulting in the formation of a two-dimensional (2D) honeycomb layer structure (Fig. 1a), which is further partitioned by the coordination between 1/3 of the bpb ligands and Co3 centers (Fig. 1b). Then, the rest 2/3 bip ligands, which coordinate with Co1 and Co2 centers, respectively, link the 2D layers together to form a three-dimensional (3D) "pillared-layer" framework (Fig. 1c). Moreover, since the large voids in one single framework, three identical and independent single frameworks are entangled with each other to generate the final three-fold interpenetrated framework of **HL-6** (Fig. 1d). The solvent accessible volume is 23.6% (526.8 $Å^3$ per unit cell volume), as estimated by PLATON [40]. Finally, topology of the framework of **HL-6** is also analyzed, and it reveals a (3,4,4)-connected 3-nodal *sqc306* type 3D net with a point symbol of $\{6{\cdot}7^2\}_2\{6^4{\cdot}7{\cdot}8\}_2\{7^4{\cdot}10{\cdot}11\}$ (Fig. S1d in Supporting information) by considering L^{3-}, Co1 or Co2, and Co3 as three-, four-, four-connected nodes, respectively.

Before property studies, the framework stability of **HL-5** and **HL-6** were further confirmed by PXRD and TGA analysis. On one hand, the PXRD patterns of the samples for both **HL-5** and **HL-6** after various treatments (solvents exchanged, dyes solution and even immersed in boiling water) agree well with the experimental and simulated ones, indicating their good phase purity and excellent framework stability against different solvents and solutions (Fig. S2 in Supporting information). On the other hand, TGA curves (Fig. S3 in Supporting information) reveal that both the two frameworks show good thermal stabilities with relatively high decomposing temperatures (**HL-5**: 400 °C; **HL-6**: 379 °C). In particular, for **HL-5**, the first step 8.7% weight loss at 30–189 °C corresponds to the departure of two free DMF molecules (calcd. 8.5 wt%), while the second loss of 6.3% at 293–343 °C means the removal of two free and four coordinated H_2O molecules (calcd. 6.2 wt%); for **HL-6**, the first obvious weight loss of 10.2% is observed at 30–169 °C, which is caused by the removal of two free H_2O and two free DMF (calcd. 10.8 wt%), and further weight loss of 4.7% was observed from 277–379 °C, which is consistent with the loss of four coordinated water molecules (calcd. 4.6 wt%). The excellent framework stability of the two MOFs provides powerful guarantee for further property studies.

Using porous materials to adsorb dyes from aqueous solutions is one of the effective methods for dyes pollutant collection. Given their hydrothermal stability, the dyes adsorption properties of the two MOFs were measured by immersing a certain amount of the samples (10 mg) in aqueous solution of dyes (MO or RhB, 5 mL, 20 mg/L). As shown in Fig. 2a, after 90 min, the orange solution of MO shaded off into colorless in the presence of **HL-6**, indicating the efficient MO adsorption of **HL-6**. Meanwhile, the absorbance peak of MO at 462 nm decreases a lot with time, and about 96.3% of total MO is adsorbed (capacity: 9.63 mg/g). However, as for RhB uptake (Fig. 2b), the solution color has almost unchanged with the absorbance peak (552 nm) slightly declined. Investigation for **HL-5** (Figs. 2d and e) reveals that it has similar dyes adsorption behaviors with **HL-6** and the MO uptake capacity is 8.0 mg/g. Moreover, a *pseudo*-first-order kinetic model (Fig. S5 in Supporting information) is evaluated for better comprehending the reaction kinetics behavior of the dye adsorption [41] and the apparent rate

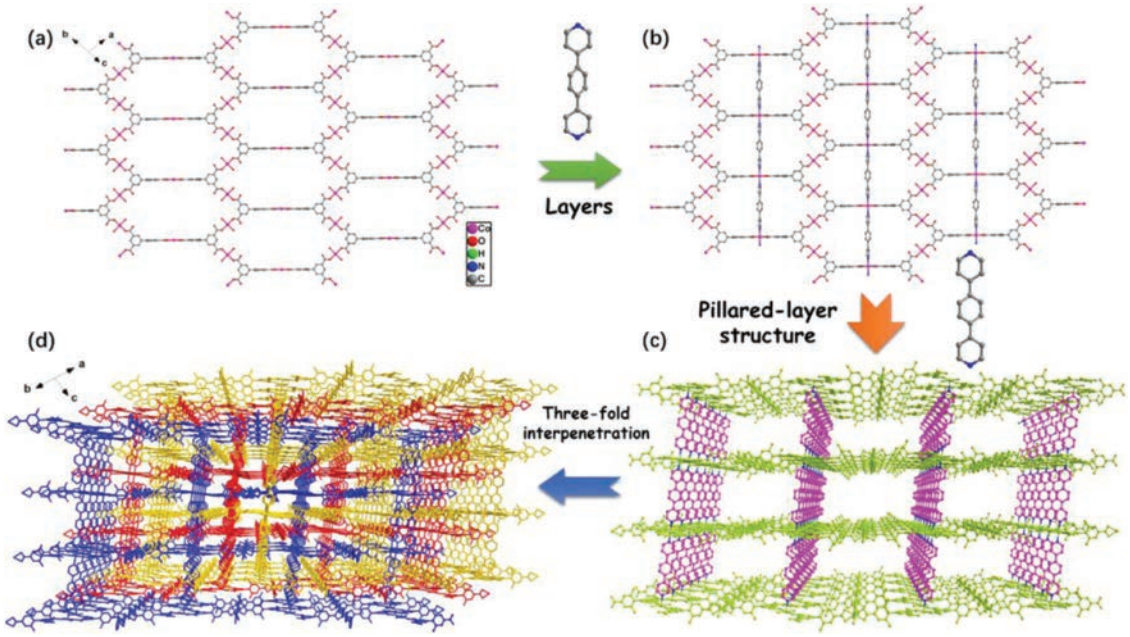

Fig. 1. Structures of the MOFs. (a, b) Formation of the 2D layer structures in **HL-6**. (c) The 3D pillared-layer framework in **HL-6**. (d) Formation of the three-fold interpenetrated 3D framework of **HL-6**.

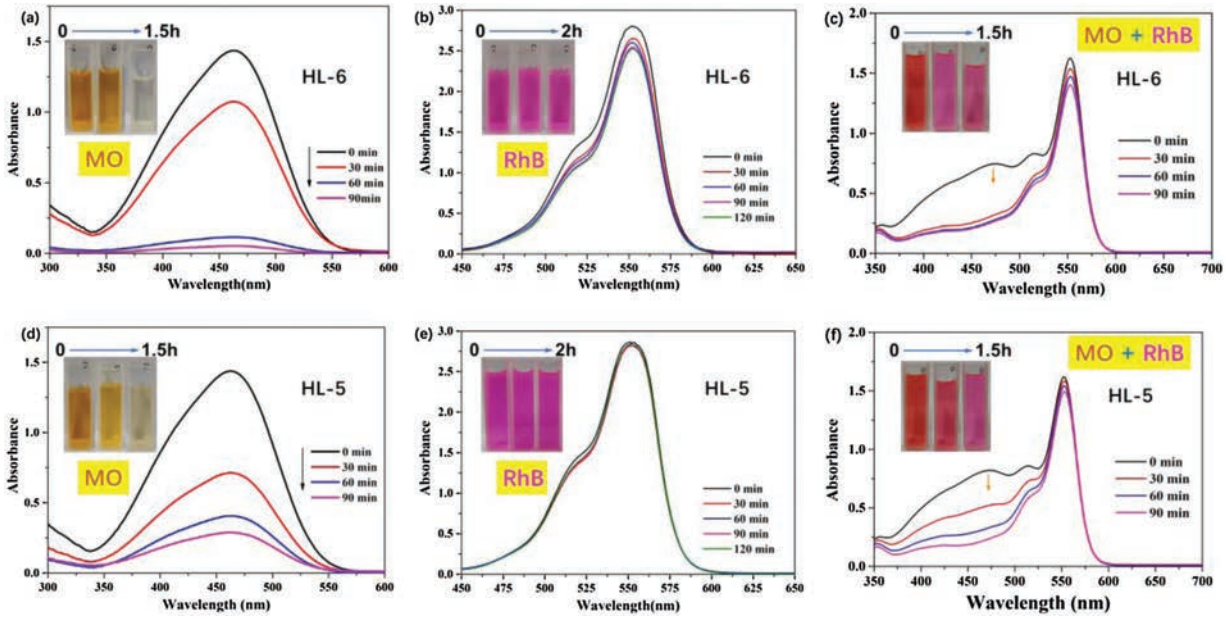

Fig. 2. UV–vis spectra and color changes during adsorption of MO and RhB in the presence of the MOFs. MO (a) and RhB (b) adsorptions for **HL-5**; MO (d) and RhB (e) adsorptions for **HL-6**. Adsorption performance of **HL-5** (c) and **HL-6** (f) in the mixture solution of MO and RhB dyes.

constants (K_a) for MO is calculated to be 1.79×10^{-2} min^{-1} for **HL-5** and 4.04×10^{-2} min^{-1} for **HL-6**.

Due to the obvious difference for MO and RhB adsorptions, dyes separation properties of **HL-5** and **HL-6** were further studied in a mixed solution (v/v = 2.5/2.5, 5 mL) as well. As shown in Figs. 2c and f, both **HL-5** and **HL-6** present good selective MO uptake over RhB. The orange red mixture gradually turns to pink which is the color of RhB, suggesting the removal of MO from the solution. Moreover, the UV–vis absorption spectra could also demonstrate that the peaks of MO at 462 nm quickly decrease with time, while the peaks of RhB at 552 nm are only slightly change. The selective MO uptake properties of the two MOFs might be attributed to the size-based sieve effect (molecular size: RhB > MO), which are caused by framework interpenetration of **HL-5** and **HL-6**.

Epoxy carbonates are widely used as reaction intermediate or solvent in some fine chemical synthesis processes. The key factor for this transformation is the adsorption and activation of the greenhouse gas CO_2. The unique features of pore structure and acidic metals have made MOFs potentially excellent catalysts. Considering the high solution stability as well as the outstanding adsorption property, catalytic transformation of CO_2 into value-added epoxy carbonates *via* cycloaddition with epoxides over the obtained MOFs were further carried out as an expand application.

The reaction was carried out under mild conditions (room temperature and 1 atm pressure). Fig. 3 shows the catalytic performance of cycloaddition of CO_2 with various epoxides over **HL-5** and **HL-6**. No product was detected without the addition of any catalysts, and about 20% yield of epoxy carbonates were obtained when adding tetrabutylammonium bromide (TBAB) as catalyst, which is consistent with the results in previous literatures. However, when adding MOFs into the reaction system in the presence of TBAB, it clearly showed an enhanced catalytic conversion rates of the products. Apparently, **HL-6** exhibited superior catalytic performance than **HL-5** under the same conditions, which should be connected with the different intensity of acidic metal site. The yield of propylene carbonate over **HL-6** is 76.27%, which is obvious higher than that of

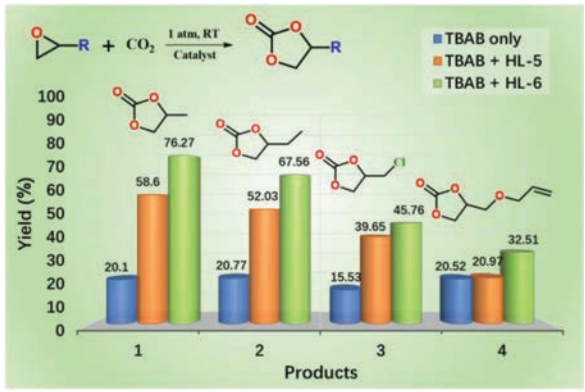

Fig. 3. Yields of propylene carbonates from cycloaddition of CO_2 and different propylene oxide with and without the two MOFs.

HL-5 and some reported catalysts (for example, the yield of propylene carbonate is 49.20%, 48% and 47.5% over HKUST-1, MOF-505 and Cu(tactmb), respectively) [42,43]. Some high yield of propylene carbonate (>80%) was also reported over some MOFs, however, excessive TBAB and/or high temperature are required during the reaction process [44,45]. In addition, the yield of epoxy carbonate decreased over both **HL-5** and **HL-6** with the increase of molecular size of epoxides substrates, which should be possibly caused by the limited diffusion of epoxides with large-sized molecules into the micropores of the MOFs. These results further indicate that the obtained MOFs could potentially be used as molecular size selective catalysts in some chemical transformations.

In summary, two isostructural Ni(II)/Co(II)-based MOFs, showing 3D (3,4,4)-connected 3-nodal *sqc306* type topology, have been synthesized and characterized. The two MOFs which are hydrothermally stable, both exhibit good selective dye adsorption of MO over RhB. Further studies reveal that both the two MOFs also show certain catalytic activity in CO_2 cycloaddition with epoxides at ambient conditions.

Declaration of competing interest

The authors declared that they have no conflicts of interest to this work.

Acknowledgments

This work was financially supported by the National Natural Science Foundation of China (NSFC, Nos. 21601028, 21902022 and 21371028), and the NSF of Shandong Province (Nos. ZR2019QB026, ZR2018LB018, ZR2016BM26 and ZR2016BL04).

Appendix A. Supplementary data

Supplementary material related to this article can be found, in the online version, at doi:https://doi.org/10.1016/j.cclet.2020.02.028.

References

[1] X.L. Zhang, Y.Z. Zhang, D.S. Zhang, B. Zhu, J.R. Li, Dalton Trans. 44 (2015) 15697–15702.
[2] B.Q. Guo, J.L. Zhao, C.Y. Wu, et al., Colloid Surf. B: Biointerfaces 177 (2019) 346–355.
[3] S.J. Ye, M. Yan, X.F. Tan, et al., Appl. Catal. B: Environ. 250 (2019) 78–88.
[4] S.S. Han, J.L. Mendoza-Cortés, W.A. Goddard III, Chem. Soc. Rev. 38 (2009) 1460–1476.
[5] Z.G. Gu, H. Fu, T. Neumann, Z.X. Xu, et al., ACS Nano 10 (2016) 977–983.
[6] Z.G. Gu, D.J. Li, C. Zheng, et al., Angew. Chem. Int. Ed. 56 (2017) 6853–6858.
[7] D. Huang, X. Wu, J. Tian, et al., Chin. Chem. Lett. 29 (2018) 845–848.
[8] Z.B. Liang, C. Qu, W.H. Guo, R.Q. Zou, Q. Xu, Adv. Mater. 30 (2018) 1870276.
[9] Q.X. Yang, S.S. Ren, Q.Q. Zhao, et al., Chem. Eng. J. 333 (2018) 49–57.
[10] D.S. Zhang, Q. Gao, Z. Chang, et al., Adv. Mater. 30 (2018) 1804715.
[11] Y.Q. Chen, Y. Tian, S.L. Yao, et al., Chem. Asian J. 14 (2019) 4420–4428.
[12] W.H. Huang, J. Ren, Y.H. Yang, et al., Inorg. Chem. 58 (2019) 1481–1491.
[13] Y.P. Li, X.H. Zhu, S.N. Li, et al., ACS Appl. Mater. Interfaces 11 (2019) 11338–11348.
[14] R.B. Lin, S.C. Xiang, H.B. Xing, W. Zhou, B.L. Chen, Coord. Chem. Rev. 378 (2019) 87–103.
[15] X.B. Liu, T. Yue, K. Qi, et al., Chin. Chem. Lett. 31 (2020) 2189–2201.
[16] S.L. Yao, S.J. Liu, X.M. Tian, et al., Inorg. Chem. 58 (2019) 3578–3581.
[17] J.D. Xiao, H.L. Jiang, Acc. Chem. Res. 52 (2019) 356–366.
[18] D.X. Xue, Q. Wang, J.F. Bai, Coord. Chem. Rev. 378 (2019) 2–16.
[19] Y.X. Ye, Z.L. Ma, R.B. Lin, et al., J. Am. Chem. Soc. 141 (2019) 4130–4136.
[20] X.F. Zhang, L. Chang, Z.J. Yang, et al., Nano Res. 12 (2019) 437–440.
[21] B. Wang, P. Wang, L.H. Xie, et al., Nat. Commun. 10 (2019) 3861.
[22] T.T. Zhu, Z.M. Zhang, W.L. Chen, Z.J. Liu, E.B. Wang, RSC Adv. 6 (2016) 81622–81630.
[23] X.L. Zhang, P.F. Liu, N. Wang, D.S. Zhang, Polyhedron 126 (2017) 83–91.
[24] L. Chen, L. Zuo, Z.X. Jiang, et al., Chem. Eng. J. 361 (2019) 559–570.
[25] Q. Yang, B. Wang, Y. Chen, Y. Xie, J. Li, Chin. Chem. Lett. 30 (2019) 234–238.
[26] L.H. Xie, X.M. Liu, T. He, J.R. Li, Chem 4 (2018) 1911–1927.
[27] Q.H. Yang, Q. Xu, S.H. Yu, H.L. Jiang, Angew. Chem. Int. Ed. 55 (2016) 3685–3689.
[28] Y.P. He, L.B. Yuan, G.H. Chen, et al., J. Am. Chem. Soc. 139 (2017) 16845–16851.
[29] D.S. Zhang, Y.Z. Zhang, J. Gao, et al., Dalton Trans. 47 (2018) 14025–14032.
[30] X.L. Zhang, J.N. Fu, D.S. Zhang, L.L. Geng, Polyhedron 146 (2018) 12–18.
[31] D.S. Zhang, Y.Z. Zhang, X.L. Zhang, et al., ACS Appl. Mater. Interfaces 11 (2019) 20104–20109.
[32] Q. Zhang, M. Wahiduzzaman, S.J. Wang, et al., Chem 5 (2019) 1337–1350.
[33] B. Wang, H. Yang, Y.B. Xie, et al., Chin. Chem. Lett. 27 (2016) 502–506.
[34] E. Barea, C. Montoro, J.A.R. Navarro, Chem. Soc. Rev. 43 (2014) 5419–5430.
[35] Z. Hasan, S.H. Jung, J. Hazard, Mater. 283 (2015) 329–339.
[36] Y.H. Pi, X.Y. Li, Q.B. Xia, et al., Chem. Eng. J. 337 (2018) 351–371.
[37] X.L. Zhang, H.L. Liu, D.S. Zhang, L.L. Geng, Inorg. Chem. Commun. 101 (2019) 184–187.
[38] Y.J. Wan, J.Q. Wan, Y.W. Ma, Y. Wang, T. Luo, Sci. Total Environ. 701 (2020) 12.
[39] M. Llunell, D. Casanova, J. Cirera, P. Alemany, S. Alvarez, SHAPE, Version 2.1, Universitat de Barcelona, Barcelona, Spain, 2013.
[40] A. Spek, J. Appl, Cryst. 36 (2003) 7–13.
[41] Y.S. Ho, G. McKay, Process Saf. Environ. 76 (1998) 332–340.
[42] W.Y. Gao, Y. Chen, Y. Niu, et al., Angew. Chem. Int. Ed. 53 (2014) 2615–2619.
[43] W.Y. Gao, C.Y. Tsai, L. Wojtas, et al., Inorg. Chem. 55 (2016) 7291–7294.
[44] G. Zhang, G. Wei, Z. Liu, S.R.J. Oliver, H. Fei, Chem. Mater. 28 (2016) 6276–6281.
[45] J. Liang, R.P. Chen, X.Y. Wang, et al., Chem. Sci. 8 (2017) 1570–1575.